

Electrochemical profile of nano-particle CoAl double hydroxide/active carbon supercapacitor using KOH electrolyte solution

Yong-Gang Wang, Liang Cheng, Yong-Yao Xia*

Chemistry Department and Shanghai Key Laboratory of Molecular Catalysis and Innovative Materials, Fudan University, Shanghai 200433, China

Received 23 December 2004; received in revised form 31 March 2005; accepted 6 April 2005

Available online 13 June 2005

Abstract

A nano-structured CoAl double hydroxide with an average particle size of 60–70 nm was prepared by a chemical co-precipitation. It was used as a positive electrode for the asymmetric hybrid supercapacitor in combination with an active carbon negative electrode in KOH electrolyte solution. The electrochemical capacitance performance of this kind of hybrid supercapacitor was investigated by means of cyclic voltammetry, electrochemical impedance spectroscopy and galvanostatic charge–discharge tests. A specific capacitance of 77 F g^{-1} with a specific energy density of 15.5 wh kg^{-1} was obtained for the hybrid supercapacitor within the voltage range of 0.9–1.5 V. The supercapacitor also exhibits a good cycling performance and keep 90% of initial capacity over 1000 cycles.

© 2005 Published by Elsevier B.V.

Keywords: CoAl double hydroxide; Activated carbon; Hybrid supercapacitor

1. Introduction

In recent years, the growing interest in supercapacitors has been stimulated by their potential application as electrical storage devices operating in parallel with the battery in an electric vehicle to transiently provide high power [1,2]. Electrochemical supercapacitors fill the gap between batteries and conventional capacitors in terms of their specific energy and specific power [3–6]. Supercapacitors have been used as small-scale energy storage devices in stationary electronics, such as memory back-up devices and solar batteries with semi-permanents charge–discharge cycle life. Recently, most researches have focused on the hybrid supercapacitor because of high energy density [7–11]. The new type hybrid electrochemical supercapacitors (HESs) are different from the electrochemical double layer capacitors (EDLCs), one electrode stores charge through a reversible nonfaradaic reaction of ions on the surface of an activated carbon or the hole of a nano-pore carbon material, and another electrode

is to utilize a reversible faradic reaction of redox reaction of metal oxides, conductivity polymer, and intercalated compounds. It is possible to obtain the high working voltage of the supercapacitors by choosing a proper electrode material. Both increase of the working voltage and high energy density of the faradic reaction electrode result in a significant increase of the overall energy density of the capacitors. Very recently, such type hybrid supercapacitor based on $\text{Ni}(\text{OH})_2$ and active carbon has been commercialized. However, it has drawback of undesirable power density due to the low conductivity of $\text{Ni}(\text{OH})_2$ [12]. On the other hand, CoOOH has high conductivity that has successfully coated on the surface of $\text{Ni}(\text{OH})_2$ to improve the conductivity of $\text{Ni}(\text{OH})_2$ in nickel-rare-metal battery. However, $\text{Co}(\text{OH})_2$ is not very stable in alkaline medium. Recently, an Al doped CoAl double hydroxide was reported to provide a potential in using as new electrode materials for supercapacitor [13].

In the present work, we for the first time introduce CoAl double hydroxide as a positive electrode to fabricate a hybrid supercapacitor in combination with an activated carbon using 6 mol L^{-1} KOH electrolyte solution. The electrochemical capacitance performance of the hybrid

* Corresponding author. Tel.: +86 21 55664177; fax: +86 21 55664177.
E-mail address: yyxia@fudan.edu.cn (Y.-Y. Xia).

supercapacitor was investigated by cyclic voltammetry (CV), electrochemical impedance spectroscopy (EIS) and galvanostatic charge/discharge test.

2. Experimental

Activated carbon was used as received without further treatment. Cobalt aluminum double hydroxide was prepared by following process. A mixed solution containing $0.2 \text{ mol L}^{-1} \text{ Co(NO}_3)_2 \cdot 6\text{H}_2\text{O}$ and $0.1 \text{ mol L}^{-1} \text{ Al(NO}_3)_3 \cdot 9\text{H}_2\text{O}$ (the mole ratio of Co/Al was 2:1) were co-precipitated in $2 \text{ mol L}^{-1} \text{ NaOH}$ solution containing $2 \text{ mol L}^{-1} \text{ Na}_2\text{CO}_3$ at 40°C , and the suspension was stirred at 70°C for 48 h. Then the precipitate was separated by centrifugation and carefully washed with distilled water. Finally, the precipitate was dried at 80°C for 12 h. The prepared compound was characterized by X-ray diffraction (XRD, Bucker D8), scanning electronic microscope (SEM, Philip XL30) and Transmission electron microscopy (TEM, Jeol JEM-2010).

The electrode of CoAl double hydroxide was prepared according to the following steps. The mixture containing 80 wt.% CoAl double hydroxide and 15 wt.% acetylene black (AB) and 5 wt.% polytetrafluoroethylene (PTFE) was well mixed, and then was pressed onto nickel grid ($1.2 \times 10^7 \text{ Pa}$) that serves as a current collector (surface is 1 cm^2). The AC electrode was prepared by the same method as the positive electrode described above, it consisted of 80 wt.% AC, 15 wt.% AB and 5 wt.% PTFE. The typical mass load of positive electrode material (CoAl double hydroxide) is 20 and 50 mg of AC negative electrode. The used electrolyte was 6 M KOH solution. Cells were usually cycled between the voltage of 0.9 and 1.5 V; the charge and discharge rate examined was 5 mA cm^{-2} , except where otherwise specified.

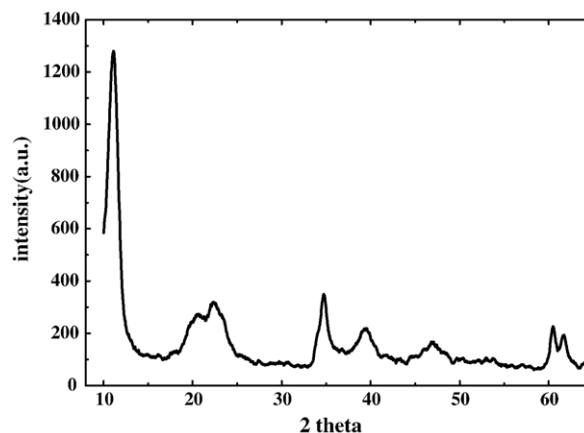


Fig. 1. X-ray diffraction pattern of the CoAl double hydroxide.

The electrochemical behavior of the resulting compound was also characterized by cyclic voltammetry and electrochemical impedance spectroscopy techniques. The experiments were carried out in a three-electrode glass cell. Platinum foil was used as a counter electrode, and Hg/HgO as a reference electrode. CV and EIS measurements were performed using a Solartron Instrument Model 1287 electrochemical interface and 1255B frequency response analyzer controlled by a computer. The frequency limits were typically set between 1000 KHz and 0.01 Hz. The AC oscillation was 10 mV. The data were analyzed by Zplot software.

3. Results and discussion

3.1. Characterization of CoAl double hydroxide

Fig. 1 shows the X-ray diffraction pattern of CoAl double hydroxide, which is consistent with the results reported

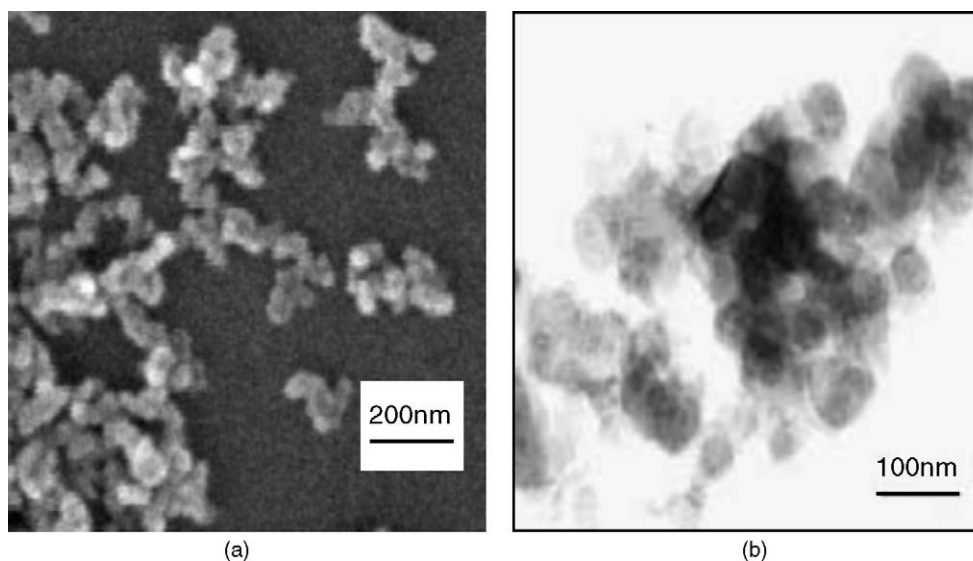
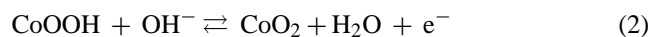
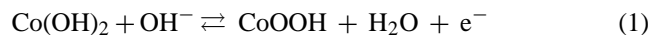


Fig. 2. SEM and TEM of CoAl double hydroxide (a) SEM and (b) TEM.

in reference [13]. The reflections of CoAl double hydroxide is very close to that of $\text{Ni}_6\text{Al}_2(\text{OH})_{16}(\text{CO}_3 \cdot \text{OH}) \cdot 4\text{H}_2\text{O}$, which suggest that this kind of materials has layered structure. Fig. 2 gives the SEM and TEM images of CoAl double hydroxide. The results in Fig. 2 clearly indicate that the prepared material has aggregated particle consisting of average particle size of 60–70 nm. By analyzing the contents of Co and Al in the precipitate solution, the concentration of residual Al^{3+} and Co^{2+} is less several ppm, we herein defined the chemical composition of CoAl double hydroxide as $\text{Co}_{0.67}\text{Al}_{0.33}(\text{CO}_3)_{0.165}(\text{OH})_2 \cdot n\text{H}_2\text{O}$ ($[\text{Co}_{1-x}\text{Al}_x(\text{OH})_2]^{x+} \cdot [\text{CO}_3^{2-}]_{x/2} \cdot [\text{H}_2\text{O}]_z, x = 0.33$) as the reference suggested [13].

3.2. Electrochemical profiles of CoAl double hydroxide and AC electrodes

We firstly applied cyclic voltammetry to detect the electrochemical reaction window and electrochemical reaction reversibility of CoAl double hydroxide in 6 mL L^{-1} KOH solution. The results are given in Fig. 3. Two redox peaks at 0.1 and 0.5 V versus Hg/HgO were clearly observed. The two redox peaks are attributed to two redox reactions as followed [14]:



We also found that the magnitude of two redox peaks between 0 and 0.2 V and that between 0.4 and 0.6 V is dependent on the Al doped content, which is associated with the content of $\text{Co}^{2+}/\text{Co}^{3+}$ in the CoAl double hydroxide. In the present work, we did not further discuss it detailed. The results in Fig. 3 also shows that CoAl double hydroxide can be charged up to 0.6 V versus Hg/HgO before the oxygen evolution, indicating the capacitance due to the redox of Co ion is fully utilized. The cyclic voltammetry of AC is also shown in Fig. 3, the curve of AC has a rectangular shape within potential win-

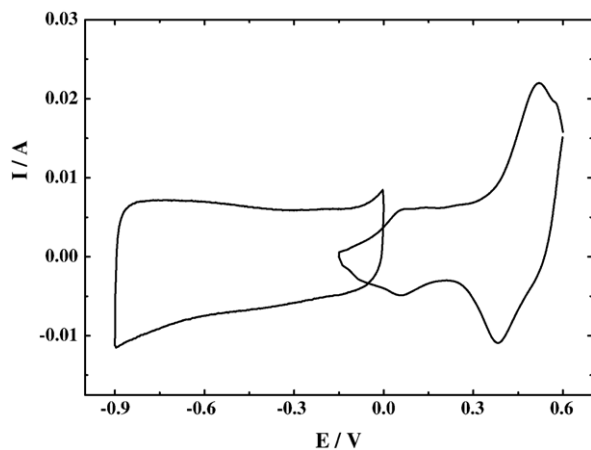


Fig. 3. Cyclic voltammetry curves of AC and CoAl double hydroxide at a scan rate of 2 mV s^{-1} . (a) AC; (b) CoAl double hydroxide.

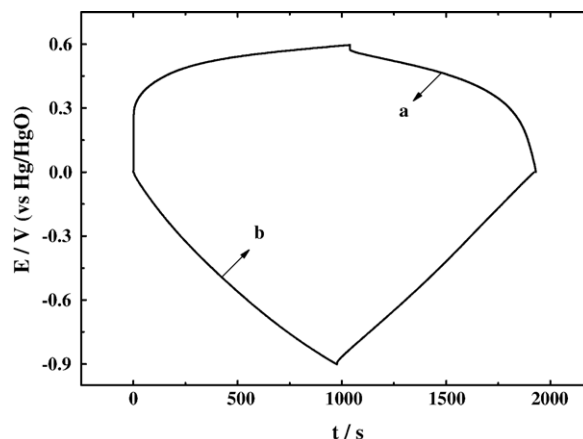


Fig. 4. Charge/discharge curves of (a) AC and (b) CoAl double hydroxide at a current density of 5 mA cm^{-2} .

dow 0 to -0.9 V (versus Hg/HgO), which is the character of double layer capacitance.

The results in Fig. 3 demonstrated that the CoAl double hydroxide can be charged/discharged between 0 and 0.6 V versus Hg/HgO, and AC between 0 and -0.9 V versus Hg/HgO. The charge–discharge curves of AC and CoAl double hydroxide at a current of 5 mA cm^{-2} are shown in Fig. 4. A perfect linear variation of the voltage was observed during the charge/discharge process of AC with a capacity of 110 F g^{-1} between 0 and -0.9 V . On the hand, CoAl double hydroxide shows a slop charge/discharge curve, it delivers a charge/discharge capacity of 360 F g^{-1} between 0.4 and 0.6 V. By comparing the delivered capacity, the optimal positive/negative mass ratio was settled around 2:5.

3.3. Capacitance performance of AC/CoAl double hydroxide hybrid supercapacitor

Fig. 5 shows CV curves of the hybrid supercapacitor with CoAl double hydroxide positive electrode and AC negative electrode in 6 M KOH solution at voltage scan rates of 2, 5

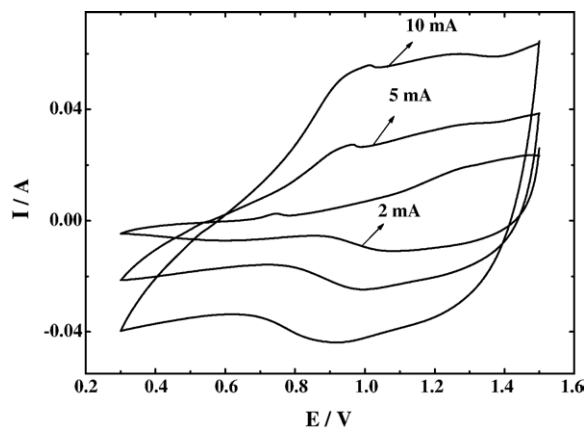


Fig. 5. CV curves of the hybrid supercapacitor at different scan rates in the voltage range from 0.3 to 1.5 V.

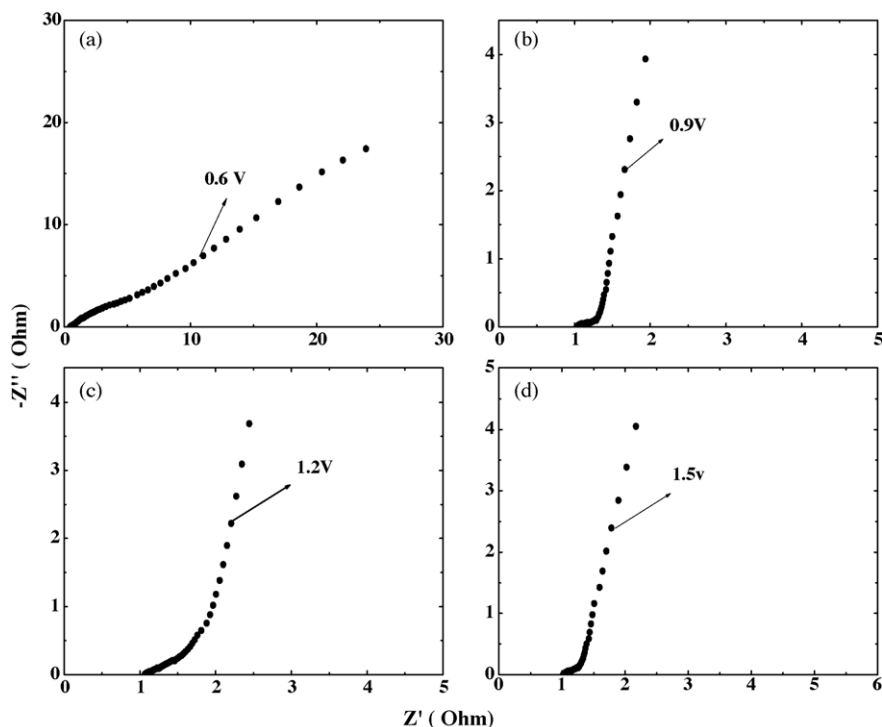


Fig. 6. Typical electrochemical impedance spectroscopy of the hybrid supercapacitor at different applied potentials.

and 10 mV s^{-1} in the potential range from 0.3 to 1.5 V. As shown in Fig. 5, the currents in the potential range from 0.3 to 0.9 V are small and the curve symmetry is poor. On the contrary, when the potential range was set between 0.9 and 1.5 V, the currents increased greatly and redox currents are symmetrical. The result of Fig. 5 indicates that the electrochemical capacitance performance of the hybrid capacitor based on CoAl double hydroxide and AC show most capacitance within certain potential window (0.9–1.5 V). This was further confirmed by electrochemical impedance spectroscopy test.

The electrochemical impedance measurements (at applied potential of 0.6, 0.9, 1.2 and 1.5 V; the frequency range is 10^5 to 10^{-2} Hz) were carried out and typical plots are shown in Fig. 6. The impedance spectrum of the cell at the potential of 0.6 V (Fig. 6 (a)) is different from that of cell at 0.9, 1.2, and 1.5 V (Fig. 6b–d). Three distinct regions are shown in Fig. 6b–d. In the low frequency region, the impedance plot of these capacitors increases and tends to become purely capacitive (vertical lines characteristic of a limiting diffusion process). In the intermediate frequency region is the 45° line that is the characteristic of ion diffusion into the electrode materials. From the point intersecting with the real axis in the range of high frequency, the internal resistances R_i of this supercapacitor is about 1Ω . However, Fig. 6a does not have this phenomenon, the slope of impedance plot does not increase and tend to 90° in the low frequency region. In brief, the result of Fig. 6 also indicates that the electrochemical capacitance performance of this hybrid supercapacitor is within certain potential window (0.9–1.5 V), which is consistent with the result of CV test.

The specific capacitance of the hybrid capacitor at different applied potentials can be evaluated from impedance test according to the following equations:

$$C_m = \frac{C}{m} = \frac{1}{m \times j \times 2\pi f \times Z''} \quad (3)$$

where C_m is the specific capacitance of the hybrid capacitor; f the frequency; Z'' the imaginary part of the impedance test; m the mass of active materials (include positive electrode and negative electrode) in the capacitor.

The specific capacitances of the hybrid capacitor at different applied potentials are shown in Table 1. The data shown in Table 1 indicates that the hybrid capacitor has electrochemical capacitance performance in the voltage range of 0.9–1.5 V.

Fig. 7 shows the galvanostatic charge–discharge curve of the hybrid supercapacitor between 0.9 and 1.5 V at currents of 5, 15 and 25 mA cm^{-2} . As shown in Fig. 7, a perfect linear variation of the voltage was observed during the charging–discharging process, which can prove that this hybrid supercapacitor has good electrochemical capacitance performance. The specific capacitance (C_m) of this hybrid supercapacitor

Table 1
The specific capacitances of the hybrid capacitor at different applied potentials evaluated from impedance tests

Capacitance at 0.6 V (F g^{-1})	13
Capacitance at 0.9 V (F g^{-1})	57
Capacitance at 1.2 V (F g^{-1})	61
Capacitance at 1.5 V (F g^{-1})	56

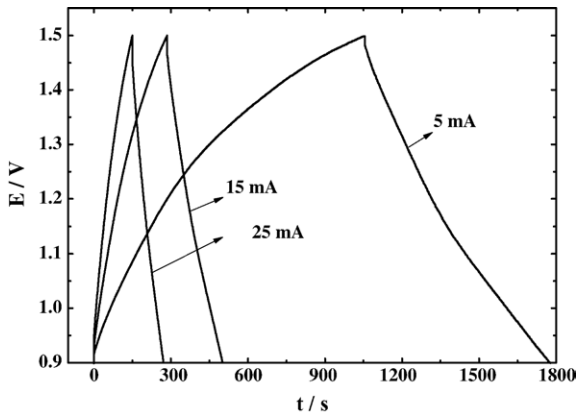


Fig. 7. Charge/discharge curves of the hybrid supercapacitor at different currents.

was calculated as follows:

$$C_m = \frac{C}{m} = \frac{It}{\Delta Vm} \tag{4}$$

where I is the current of the charge–discharge, t the time of discharge. V is 0.6 V. The m is the mass load of active materials (include positive and negative electrode). The specific power density (P) and energy density (E) of this hybrid supercapacitor were calculated as follows:

$$P = \Delta E \frac{I}{m} \tag{5}$$

$$E = pt \tag{6}$$

$$\Delta E = \frac{E_{\max} + E_{\min}}{2} \tag{7}$$

where E_{\max} is the potential at the end of charge and E_{\min} the potential at the end of discharge, I the charge–discharge current, t the discharge time and m the mass of active materials.

The specific capacitance, energy density and power density of the hybrid capacitor estimated from charge–discharge curves are shown in Table 2. A specific capacitance of 77 F g^{-1} with a specific energy density of 15.5 wh kg^{-1} can be reached. It should be noted that the specific capacitance values of this hybrid supercapacitor evaluated from impedance tests were smaller than that evaluated from charge/discharge tests.

The cycle life of the hybrid capacitor was examined at a current of 15 mA cm^{-2} was employed. The specific capac-

Table 2
The specific capacitance, power density and energy density of the hybrid capacitor at current rates of 5, 15 and 25 mA cm^{-2} evaluated from charge/discharge test

Capacitance (F g^{-1})	Energy density (wh kg^{-1})	Power density (W kg^{-1})
83	16.7	86
77	15.5	257
70	14.3	428

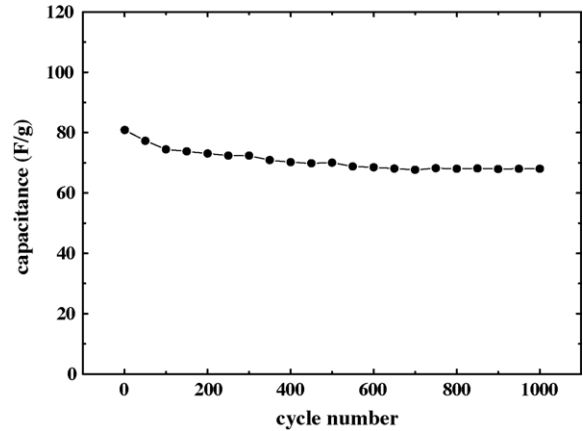


Fig. 8. Cycle-life of AC/CoAl double hydroxide hybrid supercapacitor.

Table 3
The capacitance characters evaluated from charge/discharge tests

Cycle numbers	Capacitance at $6 \text{ mA (F g}^{-1}\text{)}$	Coulombic efficiency η (%)
First cycle	77	90
Thousandth cycle	69	97

itance is shown in Fig. 8 as a function of cycle-number. It shows a slowly capacity fading at first 100 cycles, and then become constant. The charge/discharge coulombic efficiency and capacity retention were calculated by comparing the first cycle and 1000th cycle shown in Fig. 9. The results are summarized in Table 3.

The results of Table 3 indicate that the hybrid supercapacitor shows a poor charge/discharge coulombic efficiency of about 90% at first cycle. This phenomenon is consistent with the most conventional capacitor, it is partly due to the decomposition of electrolyte at the surface of electrode, but coulombic efficiency increase to 97% after 1000th cycle. Furthermore, it shows a good cycle performance. It keeps a capacitance retention of about 90% over 1000 cycles.

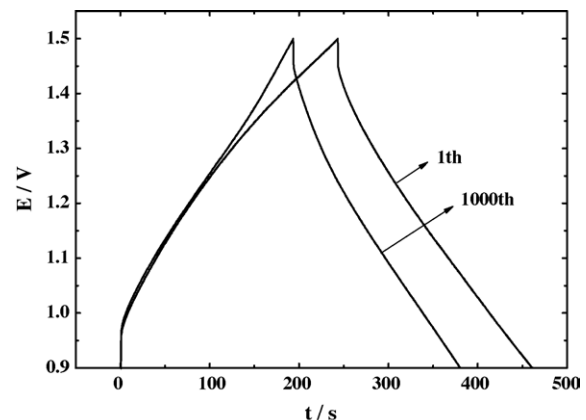


Fig. 9. Typical charge/discharge curves at different cycle numbers.

4. Conclusion

In this paper, a nano-structured CoAl double hydroxide with an average particle size of 60–70 nm was prepared by chemical co-precipitation, it delivers a capacity of 360 F g^{-1} between 0 and 0.6 V versus Hg/HgO in 6 M KOH solution. We introduced CoAl double hydroxide as a positive electrode to fabricate a hybrid supercapacitor with an activated carbon in 6 M KOH solution. The results of cyclic voltammetry and electrochemical impedance spectroscopy measurements demonstrated that the electrochemical capacitance behavior (most capacitance) was in the potential window of 0.9–1.5 V. The charge/discharge tests proves that this kind of hybrid supercapacitor has good electrochemical capacitance performance within potential range from 0.9 to 1.5 V. It delivered a specific capacitance of 77 F g^{-1} with a specific energy density of 15.5 wh kg^{-1} , and also exhibits a good cycling performance and keep 90% of initial capacity over 1000 cycles.

Acknowledgement

Financial supports from 863 program of China (No. 2003AA32302) and the nano-project of Shanghai Nanotech-

nology Promotion Center (No. 0352 nm 038) are acknowledged.

References

- [1] B.E. Conway, *Electrochemical Supercapacitors*, Plenum, New York, 1999.
- [2] R. Kotz, M. Carlen, *Electrochim. Acta* 45 (2000) 2483.
- [3] B.E. Conway, *J. Electrochem. Soc.* 138 (1991) 1539.
- [4] S.T. Mayer, R.W. Pekala, J.L. Kaschmitter, *J. Electrochem. Soc.* 140 (1993) 446.
- [5] A. Yoshida, S. Nonaka, I. Aoki, A. Nishino, *J. Power Sources* 60 (1996) 213.
- [6] Y. Kibi, T. Saito, M. Kurata, J. Tabuchi, A. Ochi, *J. Power Sources* 60 (1996) 225.
- [7] T. Brousse, M. Toupin, D. Belanger, *J. Electrochem. Soc.* 151 (2004) 614.
- [8] J.H. Park, O.O. Park, *J. Power Sources* 111 (2002) 185.
- [9] C. Arbizzani, M. Mastragostino, F. Soavi, *J. Power Sources* 100 (2001) 164.
- [10] A.D. Pasquier, I. Plitz, J. Gural, S. Menocal, G. Amatucci, *J. Power Sources* 113 (2003) 62.
- [11] A.D. Pasquier, A. Laforgue, P. Simon, *J. Power Sources* 125 (2004) 95.
- [12] R. Barnard, C.F. Randell, F.L. Tye, *J. Appl. Electrochem.* 10 (1984) 109.
- [13] M. Wohlfahrt-Mehrens, J. Schenk, P.M. Wilde, E. Abdelmula, P. Axmann, J. Garche, *J. Power Sources* 105 (2002) 182.
- [14] Z. Mi-Lin, L. Zhi-Xiang, *Chin. J. Inorg. Chem.* 18 (2002) 513.